ORIGINAL ARTICLE

Cancer Science WILEY

Small subset of Wnt-activated cells is an initiator of regrowth in colorectal cancer organoids after irradiation

Hiroko Endo[1] | Jumpei Kondo[1,2] | Kunishige Onuma[2] | Masayuki Ohue[3] | Masahiro Inoue[1,2] (iD)

[1]Department of Biochemistry, Osaka International Cancer Institute, Osaka, Japan

[2]Department of Clinical Bio-resource Research and Development, Graduate School of Medicine, Kyoto University, Kyoto, Japan

[3]Department of Surgery, Osaka International Cancer Institute, Osaka, Japan

Correspondence
Masahiro Inoue, Department of Clinical Bio-resource Research and Development, Graduate School of Medicine Kyoto University, 46-29 Shimoadachi-cho, Sakyou-ku, Kyoto, 606-8501, Japan.
Email: masa_inoue@kuhp.kyoto-u.ac.jp.

Present address
Hiroko Endo, Carnabio Sciences Inc, Hyogo, Japan

Abstract

Most colorectal cancers (CRCs) are differentiated adenocarcinomas, which maintain expression of both stemness and differentiation markers. This observation suggests that CRC cells could retain a regeneration system of normal cells upon injury. However, the role of stemness in cancer cell regeneration after irradiation is poorly understood. Here, we examined the effect of radiation on growth, stemness, and differentiation in organoids derived from differentiated adenocarcinomas. Following a sublethal dose of irradiation, proliferation and stemness markers, including Wnt target genes, were drastically reduced, but differentiation markers remained. After a static growth phase after high dose of radiation, regrowth foci appeared; these consisted of highly proliferating cells that expressed stem cell markers. Radiosensitivity and the ability to form foci differed among the cancer tissue-originated spheroid (CTOS) lines examined and showed good correlation with in vivo radiation sensitivity. Pre-treating organoids with histone deacetylase inhibitors increased radiation sensitivity; this increase was accompanied by the suppression of Wnt signal-related gene expression. Accordingly, Wnt inhibitors increased organoid radiosensitivity. These results suggested that only a small subset of, but not all, cancer cells with high Wnt activity at the time of irradiation could give rise to foci formation. In conclusion, we established a radiation sensitivity assay using CRC organoids that could provide a novel platform for evaluating the effects of radiosensitizers on differentiated adenocarcinomas in CRC.

KEYWORDS
colorectal cancer, organoid, radiation sensitivity assay, radiosensitizer, Wnt

1 | INTRODUCTION

In the normal intestine, hierarchal stem cell plasticity plays an important role in both radiation sensitivity and tissue regeneration after irradiation.[1] Two types of epithelial stem cells have been identified: active and quiescent/reserve intestinal stem cells (ISCs).[2] Active ISCs are major contributors to epithelial homeostasis, but they are highly susceptible to injury. Reserve ISCs are resistant to stress, but when active ISCs are perturbed they become activated and give rise to active ISCs.[3] Previous reports have indicated that normal intestinal

epithelial cells exhibit high plasticity for regeneration upon radiation injury.

CSCs are defined as a small subset of cells within tumors that are capable of self-renewal, differentiation to non-CSCs, and tumorigenicity. Recent studies have shown that non-CSC and CSC populations exhibit considerable plasticity, which supports the notion that bidirectional conversions can occur between these 2 compartments.[4] Most colorectal cancers (CRCs) are differentiated adenocarcinomas.[5] Thus, CRCs might preserve the original plasticity of stem cells in their hierarchy.[6] However, the role of stem cell plasticity in CRC radiosensitivity is poorly understood due to the lack of an in vitro model system. Indeed, most established cancer cell lines lose their original hierarchal differentiation.[7] Recently, organoid cultures have been developed based on both normal intestinal epithelial cells and CRC cells.[8-10] Organoid cultures can facilitate the investigation of stemness in the differentiation hierarchy induced in vitro.[11] We previously developed an efficient method for the preparation and culture of spheroids from primary CRC tissues; we named these spheroids CTOSs.[8] The main principle of the CTOS method is to maintain cell-cell contact throughout the preparation and culture process. CTOSs were able to preserve the differentiation status of original CRC tumor cells, and they also displayed tumorigenic capacity.[8,12] We recently reported that CRC CTOSs showed plasticity in their stemness properties following mechanical disruption and reformation into three-dimensional structures.[13] Reformed spheroids displayed activated Wnt signaling; moreover, suppression of the canonical Wnt pathway resulted in an attenuation of the increased stemness observed following mechanical disruption.

In the present study, we established a radiation sensitivity assay using CTOSs. We observed that a small subset of radioresistant cells emerged as foci following irradiation with sublethal doses. The pre-treatment of CRC CTOSs with histone deacetylase (HDAC) inhibitors diminished CTOS regrowth following irradiation, accompanied by the suppression of Wnt signal-related gene expression and impaired DDR. An active status of Wnt signaling was thus critical for CTOS regrowth at the time of irradiation and, therefore, Wnt inhibition sensitized CRC CTOSs to X-ray irradiation.

2 | MATERIALS AND METHODS

2.1 | Patient samples and CTOS culture

The use of human tumor tissue-derived cancer cells was conducted in accordance with protocols approved by the institutional Ethics Committees at the Osaka International Cancer Institute (1803125402) and Kyoto University (R1575). Surgical specimens or biopsy samples were obtained from Osaka International Cancer Institute, with informed consent. CTOS preparation was performed as previously described.[8,14]

2.2 | CTOS regrowth assay

For the CTOS regrowth assay, CTOSs were embedded in Matrigel Growth Factor-Reduced (GFR) (BD Biosciences) and irradiated using the AB-160 irradiator (AcroBio). A detailed protocol is described in Supplementary Materials and Methods.

2.3 | Animal studies

The animal studies were approved by the Institutional Animal Care and Use Committee of Osaka International Cancer Institute and performed in compliance with institutional guidelines. A detailed protocol is described in Supplementary Materials and Methods.

2.4 | Immunohistochemistry, in situ hybridization, and western blotting

Immunohistochemistry and western blots were performed as previously described.[14,15] Detailed protocols for immunohistochemistry, western blots, and in situ hybridization are described in Supplementary Materials and Methods.

2.5 | RT-PCR

RT-PCR was performed as previously described.[15] The GeneAmp PCR System (Thermo Fisher Scientific) was used for semi-quantitative PCR, and the Step One Real-Time PCR System (Thermo Fisher Scientific) and the Fast SYBR Green Master mix for real-time PCR. The primer sequences are shown in Table S1. Gene expression was normalized to the β-actin signal to calculate relative expression levels, using the 2ΔΔCq method.[16] All data are expressed as the mean ± SD of 3 replicates.

2.6 | Microarray analysis

Microarray hybridizations were performed at Hokkaido System Science using SurePrint G3 Human GE 8x60K v.2.0 (Agilent Technologies). Microarray data are available from the NCBI Gene Expression Omnibus with accession number GSE139995. Gene set enrichment analysis and gene ontology (GO) analyses were performed using the default settings.[17]

2.7 | Reagents

Trichostatin A was purchased from FUJIFILM Wako Pure Chemical Corporation. SAHA (Vorinostat) and XAV939 were purchased from Selleck Chemicals. All reagents were used at a final concentration of 1 μmol/L.
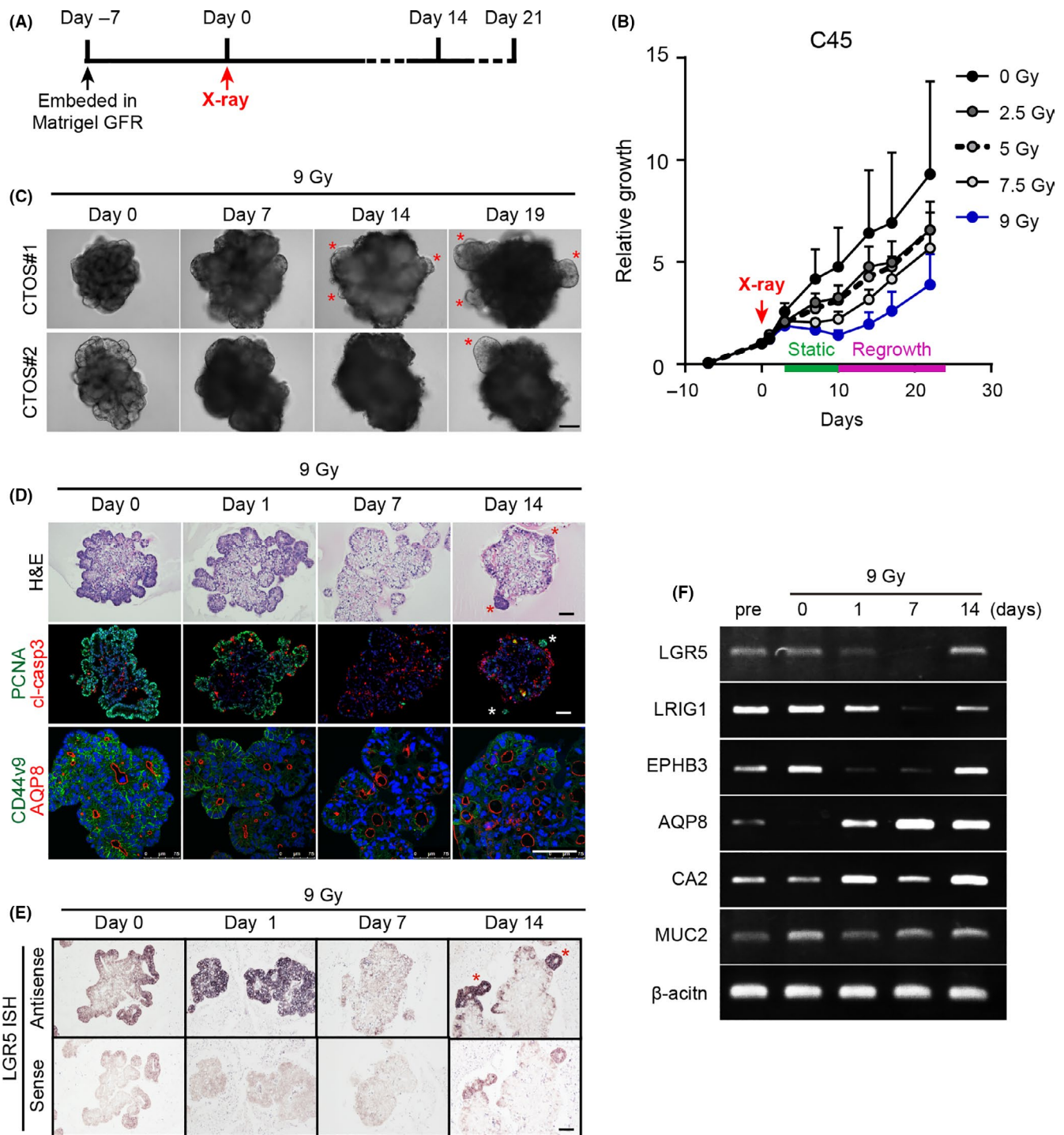
FIGURE 1 Focal regrowth of colorectal cancer organoids after high-dose X-ray irradiation. A, Experimental design. CTOSs were passaged for 1-3 d before the indicated timeline. Day −7: C45 CTOSs were embedded in Matrigel GFR and pre-cultured for 7 d; Day 0: cells were X-ray irradiated. Cells were allowed to regrow until Day 21. B, Relative growth of C45 CTOSs after X-ray irradiation. In 9-Gy irradiated CTOSs, a static phase (green bar) and a regrowth phase (magenta bar) were observed. n = 5; data are the average ± SD. C, Phase-contrast images of 2 representative C45 CTOSs, before (Day 0) and after 9-Gy irradiation. Foci of regrowth are indicated with red asterisks. Scale bar: 100 μm. D, Histological analyses of C45 CTOSs before (Day 0) and after 9-Gy irradiation. Upper panels: H&E staining, lower panels: immunofluorescence staining with antibodies against the indicated molecules; cl-casp3, cleaved caspase 3. Scale bars: 100 μm. E, In situ hybridization of *LGR5* in C45 CTOSs irradiated at 9 Gy. Foci of regrowth are indicated with red asterisks. Scale bar: 100 μm. F, Semi-quantitative RT-PCR of genes involved in intestinal stemness and differentiation. C45 CTOSs were irradiated at 9 Gy, and RNA was collected on the indicated days
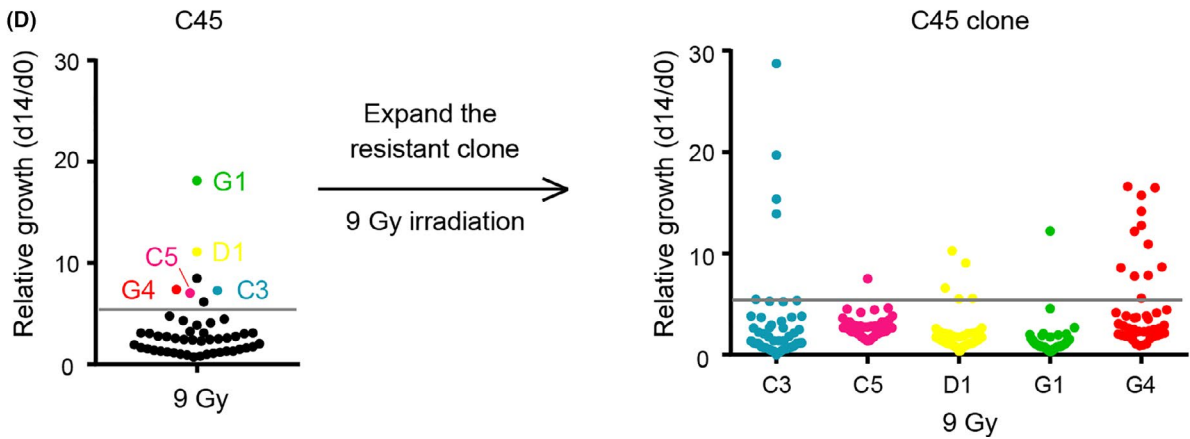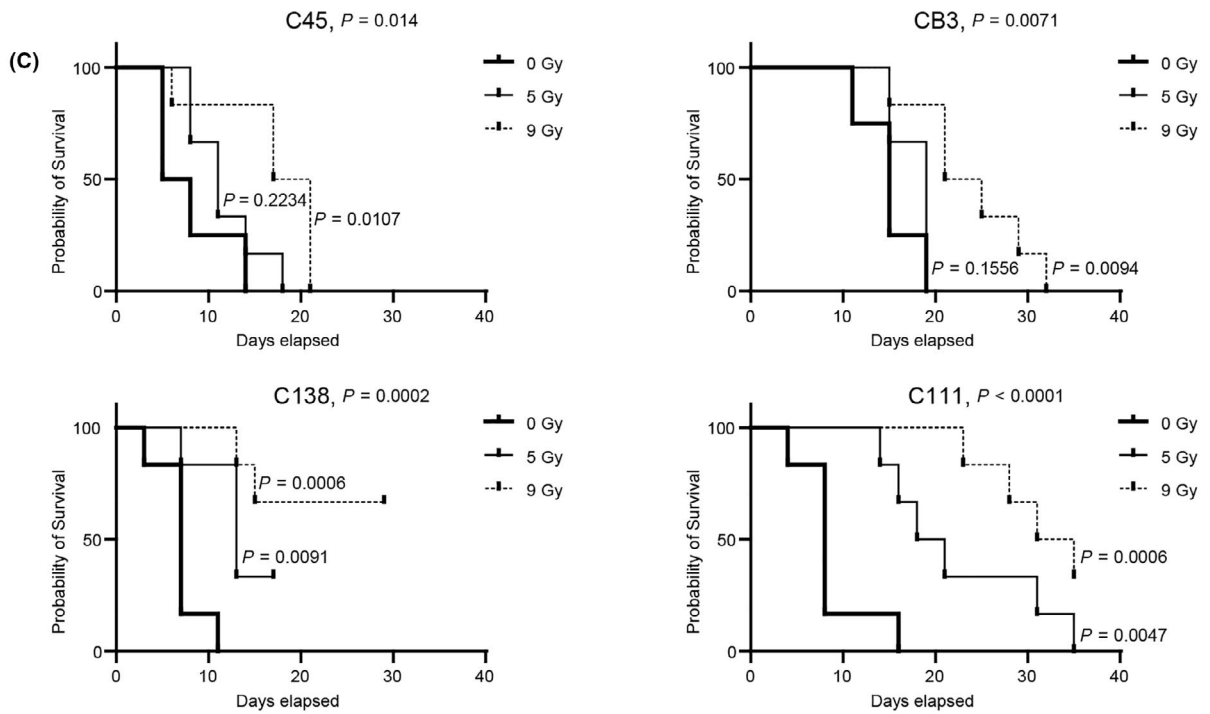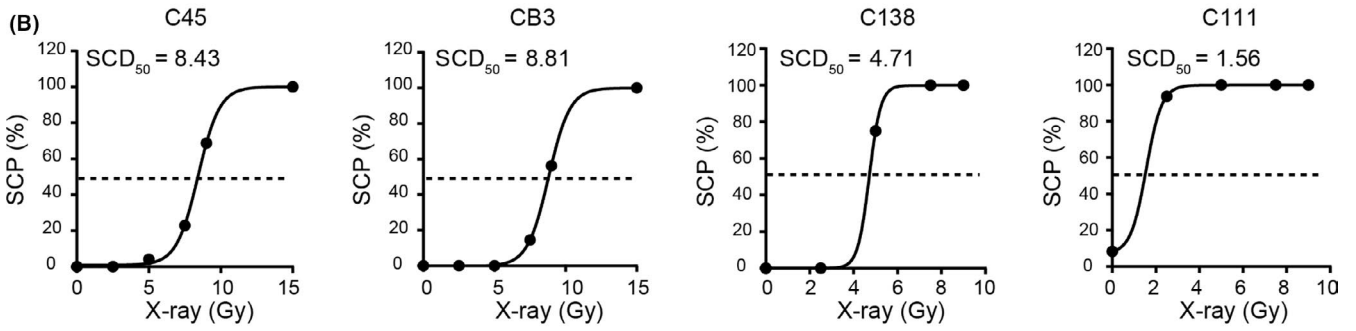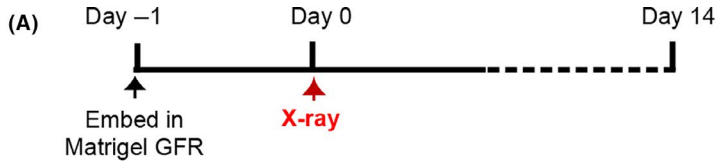
FIGURE 2 Spheroid control probability (SCP) in 4 CTOS lines. A, Experimental design. CTOSs were passaged for 1-3 d before the indicated timeline. Day −1: CTOSs were pre-cultured in Matrigel GFR overnight; Day 0: CTOSs were X-ray irradiated. CTOSs were allowed to regrow for 14 d. B, Dose-response curves show the SCP of 4 different CTOS lines, where SCP (%) = 100%, the percentage of CTOSs that regrew more than 5-fold compared with their size on Day 0. The doses that achieved half maximal spheroid control (SCD_{50}) are indicated in each graph. C, Kaplan-Meier analysis of tumor growth over 4 times more than the pre-irradiated sizes after indicated doses of irradiation for 4 CTOS lines, n = 4-6. *P*-values for entire group and pairwise comparisons between 0 Gy irradiation group are shown. D, Relative regrowth (Day 14 size/Day 0 size) of 5 clones of C45 CTOSs that were not controlled with irradiation. (*Left panel*) Five CTOSs (C3, C5, D1, G1, G4) that regrew more than 5-fold after irradiation were (*center panel*) expanded in vitro, re-plated, and irradiated again at 9 Gy. (*Right panel*) Relative regrowth after the second irradiation

2.8 | Statistical analysis

Statistical analyses were performed using GraphPad Prism 6 (GraphPad Software). The statistical significance between 2 groups was tested using the Mann-Whitney test. Regrowth rates of spheroids were compared using the chi-square test. Kaplan-Meier analysis of tumor growth was analyzed by log-rank Mantel-Cox test. A *P*-value < .05 was taken to indicate statistical significance.

3 | RESULTS

3.1 | Effect of radiation on CTOS growth, stemness, and differentiation

We first examined the time course of CTOS growth after irradiation, with the C45 line of CTOSs. Briefly, CTOSs were pre-cultured for 7 d, then irradiated at 1 of 4 different doses (2.5, 5.0, 7.5, or 9 Gy; Figure 1A,B). The retardation of CTOS growth occurred in a dose-dependent manner. After 9-Gy irradiation, CTOS size remained constant for about 14 d (static phase), then their size continued to increase at a rate similar to that seen with non-irradiated CTOSs (regrowth phase; Figure 1B). Phase-contrast imaging revealed that budding structures, with high transparency, emerged from the outer edge of the spheroids, at the turning point from the static to the regrowth phase (Day 14; Figure 1C).

Histological analyses revealed that the outer layer of the non-irradiated CTOSs at Day 0 was filled with PCNA-positive proliferating cells, which disappeared almost completely in the static phase, on Day 7 after 9-Gy irradiation (Figure 1D). At the beginning of the regrowth phase (Day 14), foci of proliferating cells reappeared in the irradiated CTOSs. Apoptotic cells, stained with antibodies against cleaved caspase-3, were scattered over the entire CTOS after irradiation. We next stained CD44v9, a putative marker of cancer stem-like cells.[18] CD44v9 expression was partially reduced on Day 1 and had almost completely disappeared in the static phase, but then reappeared in the budding structure on Day 14 (Figure 1D). Similarly, the transcripts of another stem cell marker, *LGR5*,[19] first increased on Day 1, completely disappeared by Day 7, and then finally reappeared in the budding structure on Day 14 (Figure 1E). Next, we examined the differentiation status following irradiation. The C45 CTOS line preserved the histological characteristics of a differentiated adenocarcinoma. The spheroids displayed luminal structures lined with an absorptive cell maker, AQP8 [20] (Figures 1D and S1A).

Some cells expressed other differentiation markers including synaptophysin, for endocrine cells,[21] and MUC2, for goblet cells [22] (Figure S1A). The luminal structures lined with AQP8 were maintained following irradiation (Figure 1D).

We next examined the expression of stemness/differentiation marker genes in whole C45 CTOSs, using RT-PCR (Figure 1F). The expression of stemness genes, such as *LGR5*,[19] *LRIG1*,[23] and *EPHB3*,[24] were downregulated following 9-Gy irradiation; their expression then increased at the point that regrowth started (Day 14). In contrast, the expression levels of the differentiation marker genes *AQP8*, *CA2*,[25] and *MUC2* were maintained throughout the static phase, and then *AQP8* and *CA2* expression increased.

These results indicated that, in C45 CTOSs, proliferation and stemness properties were drastically decreased following 9-Gy irradiation, but differentiation was maintained. After the static phase, regrowth foci appeared; these consisted of proliferating cells that expressed stem cell markers.

3.2 | CTOS regrowth after irradiation

To quantify the formation of regrowth foci, we used smaller CTOSs compared with those used in the experiments shown in Figure 1. In this setting, the foci appeared only in some CTOSs, following irradiation at relatively high doses. Therefore, we estimated foci formation based on the frequency of CTOS regrowth. CTOSs were plated at 1 CTOS per well in 96-well plates. Following overnight pre-culture (Figure 2A), CTOSs were irradiated at the indicated doses and cultured for an additional 14 d (Figure S2A). We used 3 CTOS lines, in addition to C45, to examine differences in radiosensitivity between the lines. The clinical information of CTOS lines are listed in Table S2. First, we evaluated the size of each CTOS (Figure S2B). We defined a 5-fold increase in size as the threshold for identifying CTOS regrowth after irradiation. Next, we assessed spheroid control probability (SCP), ie, the number of CTOSs that did not regrow at each dose, expressed as a percentage of the number of all CTOSs examined. The SCP for each CTOS line is shown in Figure 2B. The half maximal dose for achieving complete control (SCD_{50}) differed among CTOS lines. We found that CTOS lines with a high SCD_{50} showed relatively less retardation of tumor growth after irradiation in vivo (Figure 2C). The growth of each CTOS in Figure 2B is plotted in Figure S2B. These results highlighted the diversity of radiosensitivity among the cells in each CTOS line, even irradiated at the same dose.

Foci formation, which was observed in 3 lines with higher dose irradiation (Figure S1B), suggested clonal expansion; therefore, we examined whether the C45 CTOSs that regrew following 9-Gy irradiation originated from specific clones that had a fixed radioresistant phenotype. We selected 5 CTOSs that regrew following 9-Gy irradiation and individually expanded each one. Then, each CTOS was plated into 1 well of a 96-well plate, and the expanded clones were irradiated. We found that each CTOS clone showed radio-resistance similar to that displayed by the C45 CTOSs following their first irradiation (Figure 2D). This result indicated that the cells in the foci that regrew did not have a fixed resistance, instead their resistance was transient and plastic.

3.3 | Mechanical disruption increased CTOS regrowth after irradiation

The plasticity of stem cells in their hierarchy plays an important role in the radiation sensitivity of the normal intestine.[1] Therefore, we investigated whether stemness plasticity played a role in CTOS radiosensitivity. We previously reported that disruption of the 3D architecture of CTOS, including the C45 and CB3, by a shearing force of passing through a syringe needle increased the stemness of CRC cells during the CTOS reformation process. Wnt signaling played a role in the gain of stemness.[13] We examined the frequency of CTOS regrowth following 9-Gy irradiation in disrupted CTOSs. We compared "non-disrupted (ND)" CTOSs, which were cultured in suspension for 7 d after periodic passaging, with "disrupted CTOSs (D)", which were cultured for 24 h following mechanical disruption[13] (Figure 3A). The frequency of CTOS regrowth following 9-Gy irradiation was significantly higher among the disrupted CTOSs than among the ND CTOSs (Figure 3B-D). However, the growth of CTOSs was about the same between disrupted and ND CTOS when they were cultured in Matrigel without irradiation (Figure 3E). These results indicated that mechanical disruption increased the radio-resistance of CTOS.

3.4 | HDAC inhibitors suppressed CTOS regrowth following irradiation

Numerous studies have demonstrated that histone deacetylase (HDAC) inhibitors can modulate cellular responses to other cytotoxic modalities, including ionizing radiation.[26] Therefore, we next applied a radiosensitivity assay to assess the radiosensitizing effect of HDAC inhibition. C45 and CB3 CTOSs were first disrupted and then pre-treated overnight with HDAC inhibitors, either trichostatin A (TSA) or suberoylanilide hydroxamic acid (SAHA, vorinostat). At 2 h following the removal of the reagents, CTOSs were irradiated at 9 Gy (Figure 4A). We found that pre-treatment with HDAC inhibitors heavily suppressed CTOS regrowth following X-ray irradiation (Figures 4B and S3A). Pre-treatment with HDAC inhibitors alone had no effect on the growth of non-irradiated CTOSs (Figure 4C).

Histone deacetylases are reported to be involved in the DDR[27,28]; therefore, we investigated the effect of HDAC inhibition on DDR following irradiation. The phosphorylation of DDR molecules, such as BRCA1, p53, and CHK1, was abolished in CTOSs pre-treated with TSA (Figure 4D and S3B). Indeed, H2AX phosphorylation, an indicator of the DNA double-strand break response,[29] increased in duration and intensity in CTOSs pre-treated with TSA (Figure 4D-F). Histone acetylation levels were markedly increased in CTOSs following overnight treatment with HDAC inhibitors. However, at the time of irradiation, 2 h after the reagents were washed out, histone acetylation had returned to basal levels (Figure 4G). These results suggested that the increase in radiosensitivity might not have been simply due to a relaxed chromatin structure.[30] Taken together, our results suggested that one of the mechanisms of action for HDAC inhibition in CTOSs was the suppression of the DDR, as previously shown in conventional cell lines.[31]

3.5 | HDAC inhibitors targeted Wnt signaling

Based on our finding that pre-treatment with HDAC inhibitors sensitized CTOSs, we speculated that the radiosensitivity of each cell might be determined at the time of irradiation. To examine the effect of HDAC inhibitors on gene expression, we performed a microarray analysis with CTOSs pre-treated with TSA, without irradiation. GO analyses revealed that genes related to DNA repair and the G2M checkpoint were highly downregulated in CTOSs pre-treated with TSA, as previously reported (Figure 5A).[32,33] In addition, we observed increased expression of intestinal differentiation genes, such as the genes involved in protein secretion and fatty acid oxidation.

Although *Wnt* did not appear in the top-10 list of the GO analysis, we focused on Wnt target genes, because we had previously reported that mechanical disruption of CRC CTOSs increased CTOS stemness, partly due to the activation of Wnt signaling.[13] A gene set enrichment analysis showed significant enrichment of Wnt target genes in CTOSs treated with DMSO compared with these genes in CTOSs treated with the HDAC inhibitor (Figure 5B). A real-time RT-PCR analysis revealed that the expression levels of the Wnt target genes *LGR5*, *ASCL2*, and *CDX1*[34] were downregulated in CTOSs pre-treated with TSA or SAHA (with the exception that *CDX1* expression was not affected in CB3 CTOSs treated with SAHA; Figure 5C). These results indicated that pre-treatment with HDAC inhibitors suppressed the expression of genes involved in both DNA repair and the Wnt pathway.

3.6 | Wnt signaling is necessary for CTOS regrowth after radiation

We examined whether Wnt signaling played a critical role in increasing the frequency of regrowth among disrupted CTOSs. Disrupted and ND CTOSs were pre-treated overnight with a tankyrase inhibitor, XAV939. Treatment with 1 μM of XAV939 upregulated AXIN2 protein
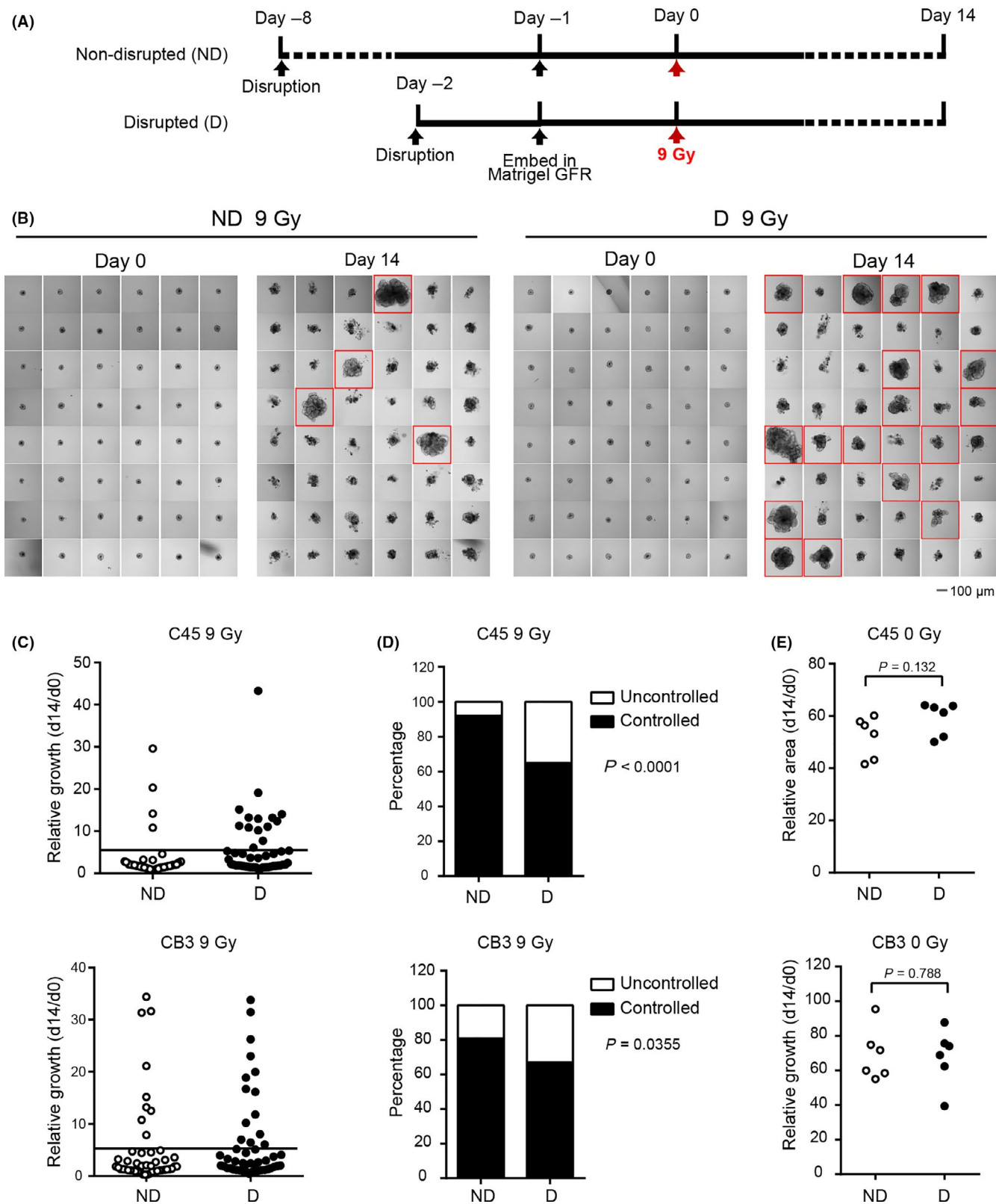
FIGURE 3 Mechanical disruption promoted radio-resistance in CRC CTOSs. A, Experimental design. Day −8: CTOSs were mechanically disrupted (non-disrupted group). Day −2: CTOSs were mechanically disrupted (disrupted group). Day −1: CTOSs were pre-cultured in Matrigel GFR overnight; Day 0: CTOSs were irradiated at 9 Gy. CTOSs were allowed to regrow for 14 d. B, Phase-contrast images of mechanically disrupted (D) or non-disrupted (ND) C45 CTOSs before (Day 0) and 14 d after irradiation at 9 Gy. The red boxes indicate uncontrolled CTOSs. C, Quantitative analysis of the experiments shown in panel B for CTOS C45 and CB3 lines. Relative growth on Day 14 is shown for all cells in each CTOS (n = 48). D, Percentages of controlled or uncontrolled cells in the CTOSs shown in panel C. E, Relative growth of non-irradiated CTOSs that were disrupted (D) or non-disrupted (ND) (n = 6 each)

(A) Day −2 ... Day −1 ... DMSO or HDACi ... Day 0 ... 2 h ... Day 14
Disruption ... Embed in Matrigel GFR ... Wash ... 9Gy

(B) C45 9 Gy — Relative growth (d14/d0); DMSO vs TSA

(C) C45 0 Gy — Relative growth (d14/d0); DMSO vs TSA; *P* = 0.675

(B) C45 9 Gy — Relative growth (d14/d0); DMSO vs SAHA

(C) C45 0 Gy — Relative growth (d14/d0); DMSO vs SAHA; *P* = 0.898

(D) DMSO pre-treat / TSA pre-treat; Time after IR (h): −, 0, 2, 4, 6; pBRCA1, pp53, pCHK1, pCHK2, pH2AX, β-actin

(E) 9 Gy; Time after IR (h): −, 0, 24, 48; pH2AX — DMSO, TSA 1 µM

(F) C45 — pH2AX foci/nuclei; DMSO: 0Gy, 9Gy 0h, 9Gy 24h, 9Gy 48h; TSA 1 µM: 0Gy, 9Gy 0h, 9Gy 24h, 9Gy 48h; *P* < 0.0001

(G) Time after wash out (h): DMSO 0, 2; TSA 1 µM 0, 2; SAHA 1 µM 0, 2; Acetyl H3 K9, Acetyl H3 K27, Acetyl H3 K14, Acetyl H3 K18, β-actin

level (Figure S4A). After the XAV939 was washed out, the CTOSs were irradiated with 9 Gy (Figure 6A). We found that the increased frequency of regrowth in disrupted CTOSs was diminished by pretreatment with the Wnt inhibitor (Figure 6B). Pre-treatment alone had no effect on the growth of non-irradiated CTOSs (Figure 6C). Pre-treatment with a porcupine homolog inhibitor, IWP-2, tended to

show similar effect to XAV939, although not statistically significant (Figure S4B).

The Wnt pathway reportedly affects the DDR[35], therefore we examined changes in DDR-related molecules. We found that the phosphorylation of DDR molecules was marginally suppressed in CTOSs pre-treated with the Wnt inhibitor (Figure 6D). In CTOSs

FIGURE 4 HDAC inhibitor pre-treatment abolished CTOS regrowth following 9-Gy irradiation. A, Experimental design. Day −2: CTOSs were disrupted. Day −1: Disrupted CTOSs were embedded in Matrigel GFR and pre-treated with DMSO, 1 μmol/L TSA, or 1 μmol/L SAHA overnight. (Day 0) After removing the reagents, CTOSs were cultured in fresh medium for 2 h, then irradiated at 9 Gy. CTOSs were allowed to regrow for 14 d. B, Relative growth of C45 CTOS pre-treated without (DMSO, black) or with TSA (green) or SAHA (red) at 14 d after 9-Gy irradiation (n = 48). C, Relative growth of non-irradiated CTOSs treated without (DMSO, black) or with TSA (green) or SAHA (red) (n = 6). D, Western blot shows expression of molecules involved in the DNA damage response at different times after irradiation (IR), as indicated, in C45 CTOSs, pre-treated with DMSO or 1 μmol/L TSA and irradiated at 9 Gy. E, Immunofluorescence images show phospho-H2AX (pH2AX) expression (red) after 9-Gy irradiation. C45 CTOSs were pre-treated with DMSO or 1 μmol/L TSA. Blue; DAPI. Scale bar = 100 μm. F, Quantitative analysis of the number of pH2AX foci per nuclei shown in panel E. N = 129-302 for each condition; data are the average ± SD G, Western blot showing acetylated histone-H3 levels in C45 CTOSs. CTOSs were pre-treated overnight with DMSO or HDAC inhibitors; then, cells were collected at 0 h or 2 h after washing out the reagents

pre-treated with XAV939, H2AX phosphorylation was increased at 2 h post irradiation compared with that in untreated CTOSs, but the duration of phosphorylation was nearly the same in both groups (Figure 6D). Conversely, pre-treatment with XAV939 strongly suppressed the expression of intestinal stemness genes such as *LGR5*, *LRIG1*, *ASCL2*, and *EPHB3*, and increased the expression of the differentiation genes *ALPI*,[36] *KRT20*,[37] *FABP1*,[38] and *AQP8* (Figure 6E). These results indicated that the increased sensitivity of CTOS following pre-treatment with a Wnt inhibitor might have been due to alterations in stemness/differentiation status, rather than alterations in the DDR.

4 | DISCUSSION

We used CRC CTOSs, which retain the differentiation status of the original differentiated adenocarcinomas,[8,12] to investigate the nature of regrowth following irradiation. We found that those cells that expressed stem cell markers mostly disappeared after high doses of radiation, which indicated that not all stem-like cells contributed to regrowth following irradiation. After a static phase, regrowth foci appeared in some CTOSs, which included *LGR5*-positive and proliferative cells. Regrowth was suppressed by HDAC inhibitors, which inhibited Wnt pathways as well as the DDR. In addition, Wnt inhibitors suppressed regrowth. These results indicated that the cells that generated regrowth foci were the cells that showed activated Wnt signaling at the time of irradiation.

Clonogenic assays have been the standard method used for evaluating radiosensitivity at the level of individual cells. In this method, the number of colonies derived from a single cell that resisted cell death by irradiation are counted, and the ratio of the number of colonies to the total number of cells examined is calculated.[39] The caveat of any clonogenic assay is that the cells must be dissociated into single cells at the beginning of the assay. Therefore, the effect of cell-cell contact on radiation sensitivity cannot be evaluated using this method. To overcome this limitation, multicellular spheroids have been used for radiosensitivity assays, mostly with conventional, established cell lines.[40] However, the growth inhibition of spheroids is not a suitable platform for studying radiosensitivity at the level of individual cells. In this study, we applied the SCP to our CTOS-based radiosensitivity assay, and focused on the nature of those cells that initiated

regrowth following high doses of radiation, which provided some, but not complete control.

According to the CSC hypothesis, only the CSC sub-population of cells is responsible for the initiation and maintenance of a tumor; therefore, these cells must be eradicated to achieve a cure. Thus, the SCP can be also defined as the probability of eradicating CSCs with a given dose of radiation.[41] We previously reported that mechanical disruption could enhance the stemness, colony forming capacity, and tumorigenicity of CRC CTOSs, and that increased Wnt activity played a critical role.[13] In the present study, we demonstrated that mechanical disruption increased the ratio of CTOSs that regrew following high-dose radiation (Figure 3) and that this effect was prevented following Wnt inhibition (Figure 6), indicating that the plasticity in the CRC stem cell hierarchy plays a role in the radiation response.

Histone deacetylase inhibitors are thought to suppress DNA repair genes related to double-strand breaks.[42,43] Indeed, as reported, pre-treating CTOSs with HDAC inhibitors strongly suppressed the expression of DDR genes (Figure 4). This finding suggested that impaired DNA repair was potentially one of the major effects of HDAC inhibition combined with irradiation (Figures 4 and 5). Conversely, HDAC inhibitors can reportedly affect Wnt signaling, either positively[44-46] or negatively,[47,48] depending on cell context. In this study, we demonstrated that HDAC inhibitors affected Wnt-related signaling in CRC CTOSs. Wnt signaling regulates stemness and differentiation.[49] The expression levels of ISC-related genes such as *LGR5*, *ASCL2*, and *CDX1*,[19] were reduced after treatment with HDAC inhibitors (Figure 5C). Considering that inhibiting Wnt signaling decreased the SCP, we concluded that altering Wnt signaling might be one of the mechanisms underlying the increased radiosensitivity induced by HDAC inhibitors.

Thus, we demonstrated that cells that were Wnt-activated at the time of irradiation were the cells that initiated regrowth. Whether these cells were CSCs or non-CSCs/differentiated cells remains to be elucidated. Since cells that expressed *LGR5* transiently disappeared following high-dose irradiation, CSCs might in general be somewhat sensitive to high-dose irradiation, with just a minor sub-population of Wnt-activated cells being resistant. Another possibility is that non-CSCs/differentiated cells were the origin of regrowth. This hypothesis was supported by the finding that the remaining cells following irradiation expressed differentiation markers in the static phase. After irradiation, a small
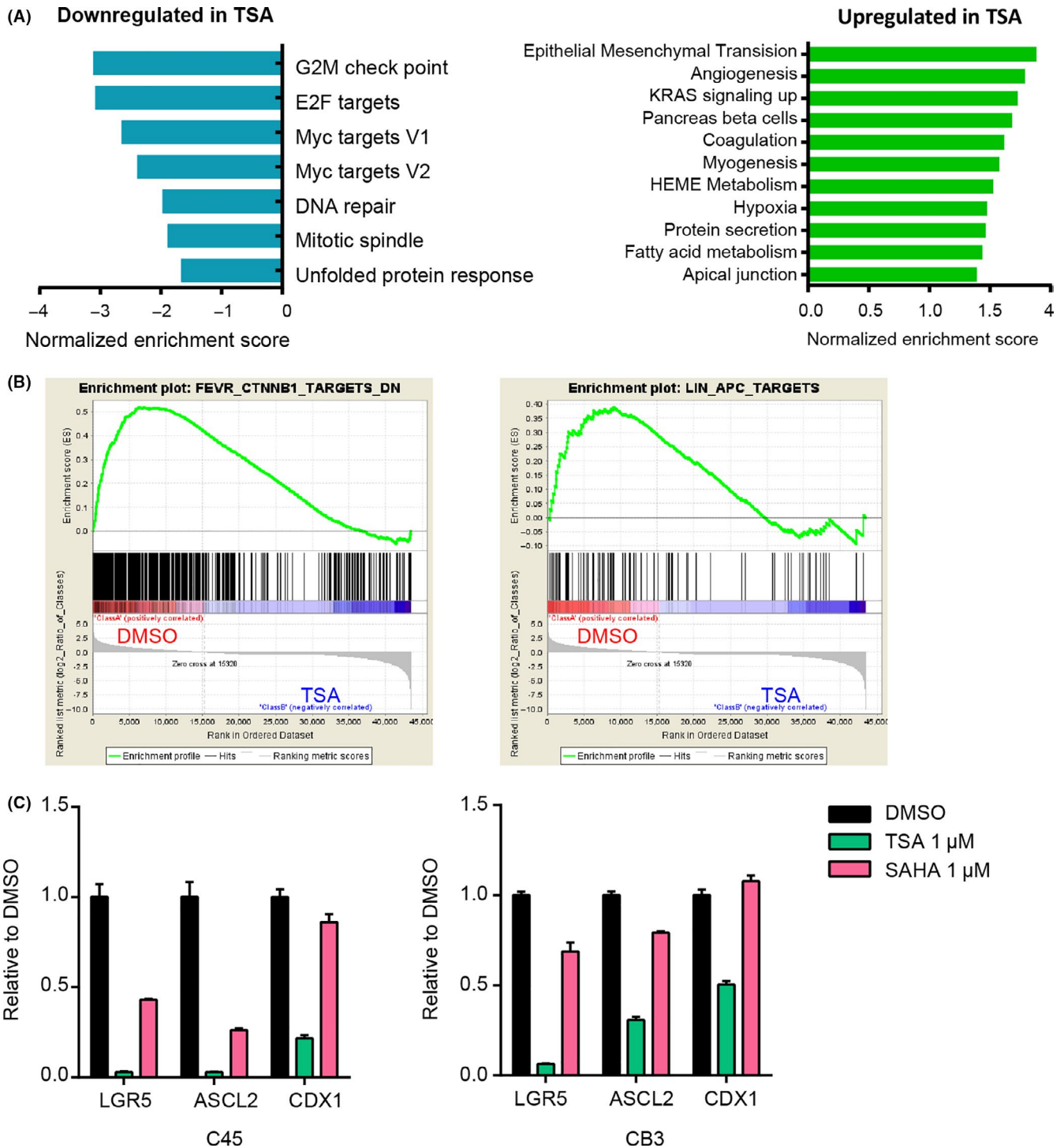
(A)

Downregulated in TSA

- G2M check point
- E2F targets
- Myc targets V1
- Myc targets V2
- DNA repair
- Mitotic spindle
- Unfolded protein response

Normalized enrichment score

Upregulated in TSA

- Epithelial Mesenchymal Transision
- Angiogenesis
- KRAS signaling up
- Pancreas beta cells
- Coagulation
- Myogenesis
- HEME Metabolism
- Hypoxia
- Protein secretion
- Fatty acid metabolism
- Apical junction

Normalized enrichment score

(B)

Enrichment plot: FEVR_CTNNB1_TARGETS_DN

Enrichment plot: LIN_APC_TARGETS

(C)

DMSO
TSA 1 μM
SAHA 1 μM

FIGURE 5 Wnt-related genes were downregulated by HDAC inhibitors. A, Microarray analysis results show gene sets in C45 CTOS that were upregulated or downregulated by TSA pre-treatment. mRNA samples were collected after the inhibitors were washed out from cells pre-treated overnight. B, Enrichment plots of gene sets in C45 CTOSs treated as described in A. (*Left panel*) Genes that showed decreased expression after deletion of β-catenin[50]; (*right panel*) genes that were upregulated with adenomatous polyposis coli overexpression.[51] C, Real-time PCR analysis results show expression levels of *LGR5*, *ASCL2*, and *CDX1* in C45 and CB3 CTOSs. CTOSs were pre-treated overnight with DMSO or HDAC inhibitors; then, washed and incubated for 2 h prior to the PCR assay

fraction of these cells might have dedifferentiated to become founder cells. Further investigation for understanding the feature of these founder cells of recurrence could contribute to the development of radiosensitization agents for CSCs. As for the clinical application, it is currently impractical to use Wnt or HDAC inhibitors for CRC treatment, meanwhile our results suggest that Wnt inhibitors could be used as a short-term treatment in combination with radiation.
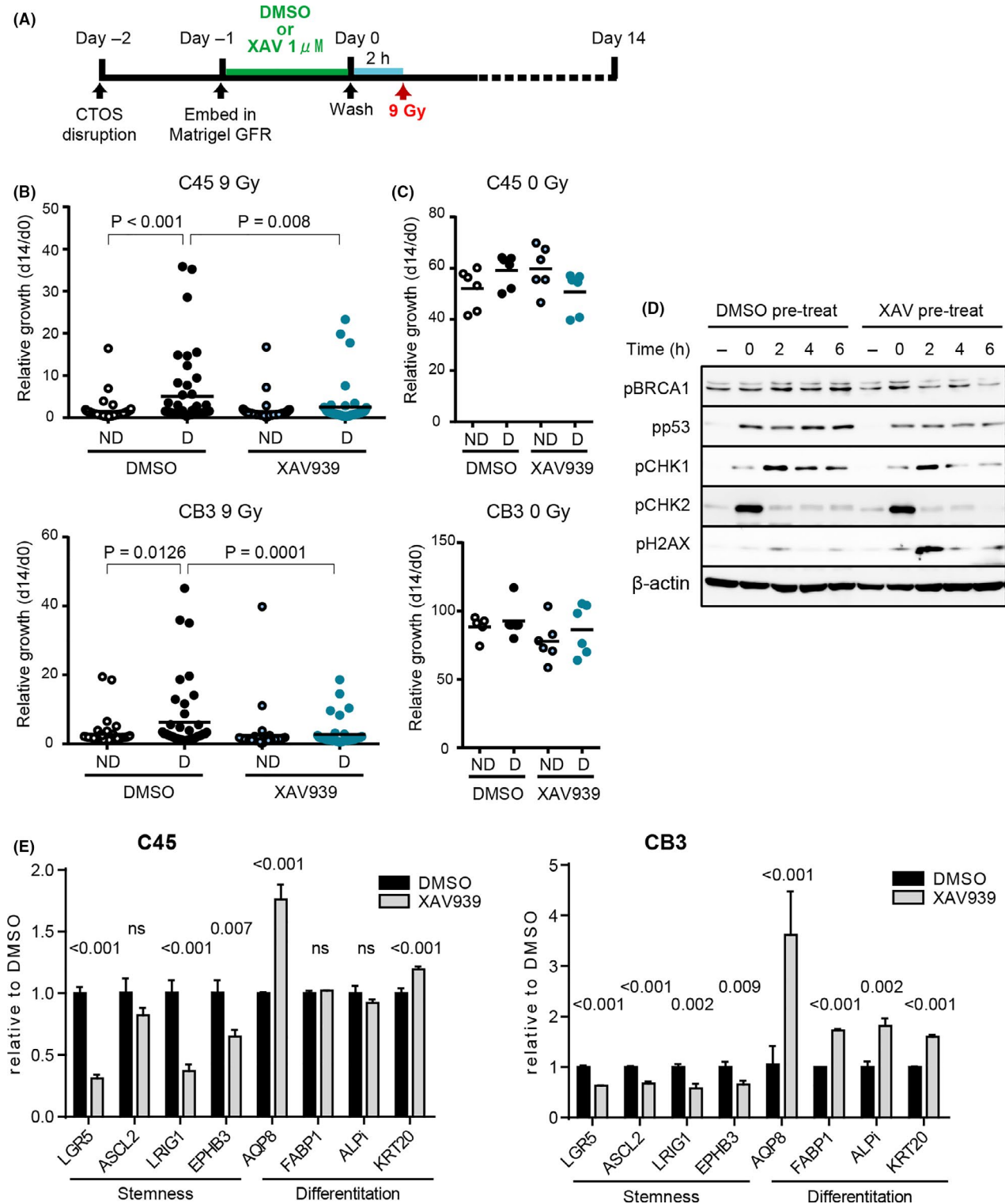
FIGURE 6 Pre-treating CTOSs with Wnt inhibitor prevented CTOS regrowth after 9-Gy irradiation. A, Experimental design. Day −2: CTOSs were mechanically disrupted (D) or non-disrupted (ND); Day −1: CTOSs were pre-treated overnight with DMSO or 1 μmol/L XAV939. Day 0: After removing the reagents, CTOSs were cultured in fresh medium for 2 h, then irradiated at 9 Gy. CTOSs were allowed to regrow for 14 d. B, Relative growth of C45 and CB3 CTOSs, pre-treated without (DMSO) or with 1 μmol/L XAV939, and tested at 14 d after 9-Gy irradiation (n = 48). C, Relative growth at Day 14 of non-irradiated CTOSs (n = 6), pre-treated without (DMSO) or with 1 μmol/L XAV939. D, Western blot shows expression of molecules involved in the DNA damage response at different times after 9Gy irradiation (IR). E, Real-time PCR of marker genes for intestinal stemness or differentiation. Mechanically disrupted C45 and CB3 CTOS were pre-cultured overnight with or without XAV939; then, RNA was extracted 2 h after removal of the reagents. The expression levels are shown relative to the DMSO controls (black) for each gene. *P*-values are indicated above each bar. ns; not significant. n = 3; data are the average ± SD

DISCLOSURE

KO, JK, and MI belong to the Department of Clinical Bio-resource Research and Development at Kyoto University, which is sponsored by KBBM, Inc. Current affiliation of HE is Carnabio Sciences Inc.

ORCID

Masahiro Inoue [iD] https://orcid.org/0000-0001-7315-026X

REFERENCES

1. Kim CK, Yang VW, Bialkowska AB. The role of intestinal stem cells in epithelial regeneration following radiation-induced gut injury. *Curr Stem Cell Rep.* 2017;3:320-332.
2. Bankaitis ED, Ha A, Kuo CJ, Magness ST. Reserve stem cells in intestinal homeostasis and injury. *Gastroenterology.* 2018;155:1348-1361.
3. Tian H, Biehs B, Warming S, et al. A reserve stem cell population in small intestine renders Lgr5-positive cells dispensable. *Nature.* 2011;478:255-259.
4. Marjanovic ND, Weinberg RA, Chaffer CL. Cell plasticity and heterogeneity in cancer. *Clin Chem.* 2013;59:168-179.
5. Fleming M, Ravula S, Tatishchev SF, Wang HL. Colorectal carcinoma: pathologic aspects. *J Gastrointest Oncol.* 2012;3:153-173.
6. Zeuner A, Todaro M, Stassi G, De Maria R. Colorectal cancer stem cells: from the crypt to the clinic. *Cell Stem Cell.* 2014;15:692-705.
7. Lee J, Kotliarova S, Kotliarov Y, et al. Tumor stem cells derived from glioblastomas cultured in bFGF and EGF more closely mirror the phenotype and genotype of primary tumors than do serum-cultured cell lines. *Cancer Cell.* 2006;9:391-403.
8. Kondo J, Endo H, Okuyama H, et al. Retaining cell-cell contact enables preparation and culture of spheroids composed of pure primary cancer cells from colorectal cancer. *Proc Natl Acad Sci U S A.* 2011;108:6235-6240.
9. Sato T, Stange DE, Ferrante M, et al. Long-term expansion of epithelial organoids from human colon, adenoma, adenocarcinoma, and Barrett's epithelium. *Gastroenterology.* 2011;141:1762-1772.
10. Fujii M, Shimokawa M, Date S, et al. A colorectal tumor organoid library demonstrates progressive loss of niche factor requirements during tumorigenesis. *Cell Stem Cell.* 2016;18:827-838.
11. Fujii M, Matano M, Toshimitsu K, et al. Human intestinal organoids maintain self-renewal capacity and cellular diversity in niche-inspired culture condition. *Cell Stem Cell.* 2018;23:787-793 e6.
12. Okuyama H, Kondo J, Sato Y, et al. Dynamic change of polarity in primary cultured spheroids of human colorectal adenocarcinoma and its role in metastasis. *Am J Pathol.* 2016;186:899-911.
13. Piulats JM, Kondo J, Endo H, et al. Promotion of malignant phenotype after disruption of the three-dimensional structure of cultured spheroids from colorectal cancer. *Oncotarget.* 2018;9:15968-15983.
14. Endo H, Okami J, Okuyama H, et al. Spheroid culture of primary lung cancer cells with neuregulin 1/HER3 pathway activation. *J Thorac Oncol.* 2013;8:131-139.
15. Endo H, Murata K, Mukai M, Ishikawa O, Inoue M. Activation of insulin-like growth factor signaling induces apoptotic cell death under prolonged hypoxia by enhancing endoplasmic reticulum stress response. *Cancer Res.* 2007;67:8095-8103.
16. Livak KJ, Schmittgen TD. Analysis of relative gene expression data using real-time quantitative PCR and the 2(-Delta Delta C(T)) Method. *Methods.* 2001;25:402-408.
17. Subramanian A, Tamayo P, Mootha VK, et al. Gene set enrichment analysis: a knowledge-based approach for interpreting genome-wide expression profiles. *Proc Natl Acad Sci U S A.* 2005;102:15545-15550.
18. Ishimoto T, Nagano O, Yae T, et al. CD44 variant regulates redox status in cancer cells by stabilizing the xCT subunit of system xc(-) and thereby promotes tumor growth. *Cancer Cell.* 2011;19:387-400.
19. Barker N, van Es JH, Kuipers J, et al. Identification of stem cells in small intestine and colon by marker gene Lgr5. *Nature.* 2007;449:1003-1007.
20. Fischer H, Stenling R, Rubio C, Lindblom A. Differential expression of aquaporin 8 in human colonic epithelial cells and colorectal tumors. *BMC Physiol.* 2001;1:1.
21. Portela-Gomes GM, Stridsberg M, Johansson H, Grimelius L. Co-localization of synaptophysin with different neuroendocrine hormones in the human gastrointestinal tract. *Histochem Cell Biol.* 1999;111:49-54.
22. Chang SK, Dohrman AF, Basbaum CB, et al. Localization of mucin (MUC2 and MUC3) messenger RNA and peptide expression in human normal intestine and colon cancer. *Gastroenterology.* 1994;107:28-36.
23. Powell AE, Wang Y, Li Y, et al. The pan-ErbB negative regulator Lrig1 is an intestinal stem cell marker that functions as a tumor suppressor. *Cell.* 2012;149:146-158.
24. Batlle E, Henderson JT, Beghtel H, et al. Beta-catenin and TCF mediate cell positioning in the intestinal epithelium by controlling the expression of EphB/ephrinB. *Cell.* 2002;111:251-263.
25. Bekku S, Mochizuki H, Takayama E, et al. Carbonic anhydrase I and II as a differentiation marker of human and rat colonic enterocytes. *Res Exp Med (Berl).* 1998;198:175-185.
26. Karagiannis TC, El-Osta A. Modulation of cellular radiation responses by histone deacetylase inhibitors. *Oncogene.* 2006;25:3885-3893.
27. Jackson SP, Bartek J. The DNA-damage response in human biology and disease. *Nature.* 2009;461:1071-1078.
28. Roos WP, Krumm A. The multifaceted influence of histone deacetylases on DNA damage signalling and DNA repair. *Nucleic Acids Res.* 2016;44:10017-10030.
29. Willers H, Gheorghiu L, Liu Q, et al. DNA damage response assessments in human tumor samples provide functional biomarkers of radiosensitivity. *Semin Radiat Oncol.* 2015;25:237-250.
30. Falk M, Lukasova E, Kozubek S. Chromatin structure influences the sensitivity of DNA to gamma-radiation. *Biochim Biophys Acta.* 2008;1783:2398-2414.
31. Newbold A, Falkenberg KJ, Prince HM, Johnstone RW. How do tumor cells respond to HDAC inhibition? *FEBS J.* 2016;283:4032-4046.
32. Laporte AN, Poulin NM, Barrott JJ, et al. Death by HDAC inhibition in synovial sarcoma cells. *Mol Cancer Ther.* 2017;16:2656-2667.
33. Ali A, Bluteau O, Messaoudi K, et al. Thrombocytopenia induced by the histone deacetylase inhibitor abexinostat involves p53-dependent and -independent mechanisms. *Cell Death Dis.* 2013;4:e738.
34. Lickert H, Domon C, Huls G, et al. Wnt/(beta)-catenin signaling regulates the expression of the homeobox gene Cdx1 in embryonic intestine. *Development.* 2000;127:3805-3813.
35. Karimaian A, Majidinia M, Bannazadeh Baghi H, Yousefi B. The crosstalk between Wnt/beta-catenin signaling pathway with DNA damage response and oxidative stress: Implications in cancer therapy. *DNA Repair (Amst).* 2017;51:14-19.

36. Shin J, Carr A, Corner GA, et al. The intestinal epithelial cell differentiation marker intestinal alkaline phosphatase (ALPi) is selectively induced by histone deacetylase inhibitors (HDACi) in colon cancer cells in a Kruppel-like factor 5 (KLF5)-dependent manner. *J Biol Chem*. 2014;289:25306-25316.

37. Moll R, Zimbelmann R, Goldschmidt MD, et al. The human gene encoding cytokeratin 20 and its expression during fetal development and in gastrointestinal carcinomas. *Differentiation*. 1993;53:75-93.

38. Levy E, Menard D, Delvin E, et al. Localization, function and regulation of the two intestinal fatty acid-binding protein types. *Histochem Cell Biol*. 2009;132:351-367.

39. Franken NA, Rodermond HM, Stap J, Haveman J, van Bree C. Clonogenic assay of cells in vitro. *Nat Protoc*. 2006;1:2315-2319.

40. Southerland RM. The multicellular spheroid system as a tumor model for studies of radiation sensitizers. *Pharmac Ther*. 1980;8:105-123.

41. Dhawan A, Kohandel M, Hill R, Sivaloganathan S. Tumour control probability in cancer stem cells hypothesis. *PLoS One*. 2014;9:e96093.

42. Cornago M, Garcia-Alberich C, Blasco-Angulo N, et al. Histone deacetylase inhibitors promote glioma cell death by G2 checkpoint abrogation leading to mitotic catastrophe. *Cell Death Dis*. 2014;5:e1435.

43. Zhao J, Xie C, Edwards H, Wang G, Taub JW, Ge Y. Histone deacetylases 1 and 2 cooperate in regulating BRCA1, CHK1, and RAD51 expression in acute myeloid leukemia cells. *Oncotarget*. 2017;8:6319-6329.

44. Bordonaro M, Lazarova DL, Augenlicht LH, Sartorelli AC. Cell type- and promoter-dependent modulation of the Wnt signaling pathway by sodium butyrate. *Int J Cancer*. 2002;97:42-51.

45. Lazarova DL, Bordonaro M, Carbone R, Sartorelli AC. Linear relationship between Wnt activity levels and apoptosis in colorectal carcinoma cells exposed to butyrate. *Int J Cancer*. 2004;110:523-531.

46. Shieh JM, Tang YA, Hu FH, et al. A histone deacetylase inhibitor enhances expression of genes inhibiting Wnt pathway and augments activity of DNA demethylation reagent against nonsmall-cell lung cancer. *Int J Cancer*. 2017;140:2375-2386.

47. Simmons GE Jr, Pandey S, Nedeljkovic-Kurepa A, Saxena M, Wang A, Pruitt K. Frizzled 7 expression is positively regulated by SIRT1 and beta-catenin in breast cancer cells. *PLoS One*. 2014;9:e98861.

48. Peiffer L, Poll-Wolbeck SJ, Flamme H, Gehrke I, Hallek M, Kreuzer KA. Trichostatin A effectively induces apoptosis in chronic lymphocytic leukemia cells via inhibition of Wnt signaling and histone deacetylation. *J Cancer Res Clin Oncol*. 2014;140:1283-1293.

49. Anastas JN, Moon RT. WNT signalling pathways as therapeutic targets in cancer. *Nat Rev Cancer*. 2013;13:11-26.

50. Fevr T, Robine S, Louvard D, Huelsken J. Wnt/beta-catenin is essential for intestinal homeostasis and maintenance of intestinal stem cells. *Mol Cell Biol*. 2007;27:7551-7559.

51. Lin YM, Ono K, Satoh S, et al. Identification of AF17 as a downstream gene of the beta-catenin/T-cell factor pathway and its involvement in colorectal carcinogenesis. *Cancer Res*. 2001;61:6345-6349.

SUPPORTING INFORMATION

Additional supporting information may be found online in the Supporting Information section.